Insights into Photosensitized Reactions for Upgrading Lignin

ACS Sustainable Chemistry & Engineering

pubs.acs.org/journal/ascecg

Research Article

Insights into Photosensitized Reactions for Upgrading Lignin

Alexander Riddell, Jonna Hynynen, Francisco Baena-Moreno, Abdenour Achour, Gunnar Westman, Jim Parkås, and Diana Bernin*

Cite This: *ACS Sustainable Chem. Eng.* 2023, 11, 4850−4859

Read Online

ACCESS | Metrics & More | Article Recommendations | Supporting Information

ABSTRACT: The conversion of lignin into valuable chemical products is important for the shift away from the petrochemical industry toward a more sustainable system of biorefineries. However, the recalcitrance and heterogeneity of lignin have made its selective depolymerization a difficult task. Photochemical methods of lignin conversion are being investigated because of the potential to operate photoreactors at milder temperatures and pressures than thermal methods and to achieve efficient reaction pathways. Furthermore, light-driven reactions facilitate reaction pathways that cannot be accessed by conventional/thermal methods. Most of the current research focuses on photocatalytic methods, which are interesting due to their potentially high selectivity, but come with the disadvantage of catalyst costs and separation requirements. In this work, we continue our investigation into the use of ultraviolet light-emitting diodes, which aims to utilize the advantages of photochemistry, while avoiding the use of expensive catalysts. Photosensitizers can participate in energy transfer, electron transfer, and hydrogen abstraction in photochemical reactions. Here, we investigated the effects of a common photosensitizer, benzophenone, on the photochemical conversion of lignin, and 2-(benzyloxy)phenol (2BP), a compound with an ether bond between two aromatic units. We monitored the conversion reactions using complementary techniques of ^{1}H nuclear magnetic resonance (NMR), diffusion NMR, and in situ Fourier transform infrared (FTIR) spectroscopy. For 2BP, the reactions with benzophenone progressed slower and without a difference in the final product formation. However, several differences were observed in photoreactions utilizing Kraft lignin and benzophenone compared to those without benzophenone. For example, a faster decay of the ^{1}H NMR peak corresponding to aromatic/phenolic protons and different changes in the shape of methoxy peaks were observed, indicating the formation of different products. This work demonstrates that benzophenone participates in the photoreactions of Kraft lignin and that the photoreactions of Kraft lignin and 2BP are different. Depolymerization of lignin into smaller fragments was confirmed with diffusion NMR, both with and without the photosensitizer.

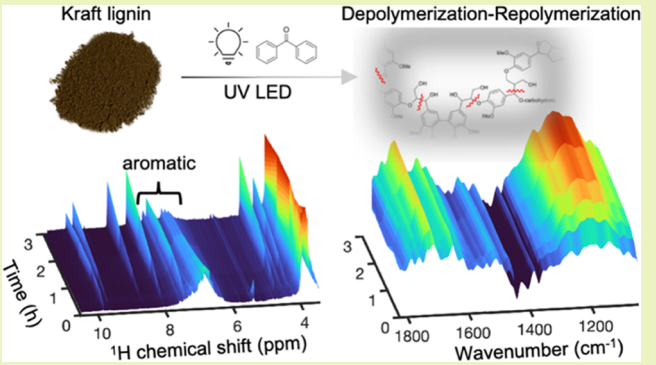

KEYWORDS: *lignin, photochemistry, valorization, biobased chemicals, photosensitization*

INTRODUCTION

The use of technical lignin to produce biobased chemicals offers a promising opportunity to valorize lignin in a circular and biobased economy. Emitted photons from light-emitting diodes (LEDs) could be used to break the linkages between the aromatic rings. The use of LEDs could potentially be an energy-efficient process for turning technical lignin into smaller fragments. This conversion process, or reduction of molecular weight for further processing, would be very attractive to the forestry industry and other industries. Lignin is the most abundant source of aromatic compounds in nature and is the second most abundant biopolymer behind cellulose.[1] After separation from cellulose in the pulping process, most technical lignin is burned for process heat. Additionally, forestry byproducts like woodchips and sawdust contain around 20−30 wt % lignin. Utilization of lignin to produce aromatics and other valuable compounds would assist the transition from a fossil-based economy to a biobased economy.[1]

The heterogeneity of lignin's structure together with its chemical recalcitrance make lignin very difficult to selectively break down. Photochemical conversion of lignin may improve selectivity toward desired products and would replace energetically demanding high-temperature, high-pressure reactors. Photochemical processes have several potential advantages over thermal reactions including selective activation of reactants, low thermal load on the reaction system, and reaction pathways that are not accessible in the ground state.[2,3] Heterogeneous photocatalysis has been used for lignin

Received: January 6, 2023
Revised: March 8, 2023
Published: March 15, 2023

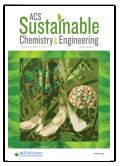

degradation in wastewater treatment.[4,5] For the conversion of lignin into valuable chemicals, the concentration of lignin in the reaction would be much higher than in the wastewater processes. Additionally, lignin would compete with catalyst particles for light absorption. Several reviews of heterogeneous photocatalysis for lignin valorization are available.[4,6,7]

There has also been work toward homogeneous photocatalysis of lignin, motivated by the potential for higher selectivity through tailored selection of metal ions and ligands.[6] However, work performed in this area of research is limited to the conversion of lignin model compounds. Unfortunately, the use of organometallic homogeneous catalysts for upgrading lignin-based byproduct streams is not yet economically feasible due to the high cost of the catalyst and its recovery. Photosensitizers can be considered an alternative to photocatalysts, and are a topic of ongoing research in sustainable synthesis.[8]

Due to its conjugated π systems, lignin contains chromophores which give a high absorptivity in the ultraviolet and visible spectrum. Research on lignin valorization often emphasizes the selective cleavage of the C−O−C and C−C bonds that link the aromatic monomers,[4,9] to be achievable through photolysis. Hynynen et al. demonstrated that UVC light depolymerized lignin extracted from sawdust without the use of photocatalysts.[10] A deeper understanding of this photochemical system is needed to determine whether photolysis can efficiently depolymerize lignin to produce valuable products.

Despite the advantages of performing reactions without catalysts or reagents using UV light, these reactions often have poor product yields and quantum efficiencies. This is partly due to short excited-state lifetimes.[11] Triplet states are of particular interest when investigating the reactivity of lignin because triplet states (denoted T_1 for the first triplet state above the ground state) can have much longer lifetimes than the excited singlet states (S_1). In the T_1 state, the excited electron and the electron at the ground level have the same spin (either both up or both down). This means that relaxation to the ground state is a "forbidden transition" and that the excited electron must undergo delayed fluorescence to return to the ground state.[3]

Photosensitizers like benzophenone can increase the population of T_1 excited states through energy transfer.[11,12] When benzophenone absorbs a photon emitted below 380 nm, a nonbonding electron from oxygen is promoted to the π^* antibonding orbital (an n−π^* transition). Since the ground-state energy level is left with one electron, it behaves like an electrophilic radical and can abstract hydrogen from another molecule. The electron in the antibonding orbital acts as a nucleophile.[3] Benzophenone has a high quantum yield for the population of triplet states. Intersystem crossing occurs very quickly (~10 ps), so triplet states are the most relevant in benzophenone photochemistry.[3] Scheme 1 presents the hypothesized pathways of hydrogen abstraction using benzophenone for acetonitrile (the solvent used in this work), lignin, and 2-(benzyloxy)phenol, a compound with an ether bond connecting two aromatic rings. The fourth line of Scheme 1a shows a benzyl radical and a phenoxy radical as potential intermediates. Both radicals are resonance-stabilized, but their relative rates of formation are unknown.

The extent that benzophenone would abstract hydrogen directly from these substrates is unknown and may, in this case, be less probable due to the relative concentration of the solvent, acetonitrile, being much greater than the lignin concentration (1 g/L). Forsskåhl et al. reasoned in their study of photosensitized lignin model compound oxidation that the influence of direct hydrogen abstraction is probably lower than the influence of singlet oxygen sensitization due to the reaction rates being much higher for carbonyl-sensitized reactions in the presence of oxygen than without oxygen.[14]

Scheme 1. (a) Hypothesized Possibilities for Hydrogen Abstraction from (2nd Row) Acetonitrile, (3rd Row) a Lignin Aromatic Unit, and (4th Row) a 2BP Molecule. (b) Possible Initiation of a Chain Scission Mechanism Involving Lignin Following Hydrogen Abstraction, Based on a Diagram from Taylor et al.[13]

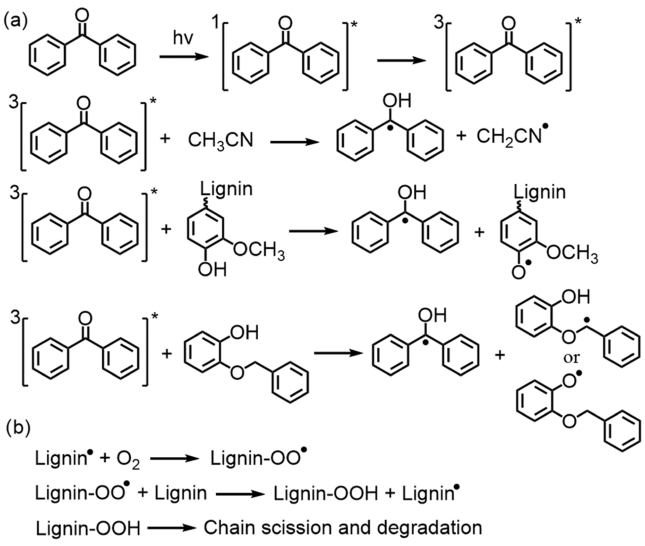

Hydrogen abstraction has been used as a strategy in other works related to lignin. For example, in the work by Luo et al., a 10% yield of aromatic monomers was obtained by hydrogen abstraction from the C_αH−OH group of poplar lignin using a $ZnIn_2S_4$ catalyst.[15] Another example is the use of the persulfate radical ($SO_4^{•-}$) for the preoxidation of a model compound for the β-O-4 lignin linkage through hydrogen abstraction.[16] Hydrogen abstraction from the β carbon was also found by Wang et al. to be the rate-determining step for C−C bond cleavage adjacent to lignin ketones during their catalytic depolymerization of lignin.[17] Additionally, hydrogen abstraction can create radicals on polymers, which can undergo chain scission reactions upon reactions with molecular oxygen.[13,18] However, creation of radicals on lignin can also lead to undesired repolymerization.[19] Hypothesized mechanisms for hydrogen abstraction and chain scission are shown in Scheme 1. Although it is difficult to assess the relevance of Scheme 1b to our work, the importance of hydrogen abstraction in adjacent research areas motivates the investigation of benzophenone in lignin photochemistry.

The role of reactive oxygen species (ROS) is of great importance for lignin photochemistry. In heterogeneous photocatalysis, molecules can be oxidized by the hydroxyl ($OH^•$) and superoxide ($O_2^{•-}$) radicals which are formed from the holes and photoinduced electrons on the catalyst surface. Other types of ROS include singlet oxygen ($^1\Delta_g$) and H_2O_2. The $^1\Delta_g$ state has a weak emission at 1270 nm and is located about 96 kJ/mol above the ground state.[3] It is typically formed via energy transfer from other molecules, for example, from photosensitizers. Although benzophenone is not particularly

https://doi.org/10.1021/acssuschemeng.3c00097
ACS Sustainable Chem. Eng. 2023, 11, 4850−4859

efficient for this purpose, singlet oxygen can be formed through energy transfer from the triplet state of benzophenone.[20] Due to the electrophilic nature, singlet oxygen will react with electron-rich groups, such as the aromatic structures in lignin.[21] H_2O_2 participates in many types of thermal and photochemical reactions, and is often applied in wastewater treatment for oxidation of organic compounds, including lignin.[14,22−24] The oxidation potentials, electronic states, and electrophilic/nucleophilic character will differ depending on the reactive oxygen species. Products formed from the oxidation of organic compounds can differ depending on the concentration of ROS.[4]

Neumann et al. performed a series of experiments to understand lignin photooxidation using flash photolysis and continuous illumination techniques with the addition of quenchers, filters, and quinones.[25,26] They observed quinoid structures and reported on the formation of phenoxy radicals due to hydrogen abstraction of phenols by molecular oxygen. In the case of reactions with benzophenone, the excited triplet benzophenone could abstract phenolic hydrogen. Additionally, Neumann et al. found that although singlet oxygen does not participate in the initiation of degradation, it does participate in the formation of final products. A photosensitizer approach that relies on generation of many triplet states could face difficulties due to triplet−triplet annihilation.[3] Introducing carbocation radicals on lignin could lead to repolymerization of lignin radical intermediates.[19]

The impact of the photosensitizer, benzophenone, on photochemical reactions of 2-(benzyloxy)phenol (2BP) and softwood Kraft lignin was evaluated by comparing reactions with and without photosensitizer. The compound 2BP is of interest because it contains an ether bond between two aromatic rings. The use of 2BP, which is a simpler molecule than lignin, enabled identification of the formed products. For our lignin sample, a softwood lignin was chosen because of its importance in Swedish pulp and paper manufacturing.[27] The variation of irradiation time and the effect on reaction products were monitored and analyzed using nuclear magnetic resonance (NMR), gas chromatography−mass spectrometry (GC-MS), and in situ Fourier transform infrared (FTIR) spectroscopy. Furthermore, comparison between photosensitized and nonphotosensitized photoreactions could provide a better understanding of the effects of hydrogen abstraction and triplet sensitization on lignin photoreactions, enabling the tuning of photoreactions of lignin for valorization.

MATERIALS AND METHODS

Materials. 2-Benzyloxy phenol (2BP) (purity >96%), benzophenone (purity 99%), deuterated acetonitrile (purity ≥99.8%), and dimethyl sulfoxide (DMSO) were purchased from Sigma-Aldrich. Lignoboost, a softwood Kraft lignin from spruce (*Picea abies*) and pine (*Pinus sylvestris*), was provided from Bäckhammar mill in Sweden. Acetonitrile (MeCN) was purchased from Fisher Chemical (purity ≥99.5%).

Solutions for photoreactions were made by mixing 30 mg of either Kraft lignin or 2BP with 30 mL of MeCN. For the photoreactions with the photosensitizer, 30 mg of benzophenone was additionally added. The contents were mixed by stirring with a magnetic stirrer for about 30 min to ensure full dissolution.

Photoreactor. All photoreactions were performed using a flow reactor setup with photons of 280 nm and an incident light intensity of $\sim 3 \times 10^{-5}$ photons L^{-1} s^{-1} described by Riddell et al.[28] The reactor has 24 LEDs (DUV 280 SD356, Roithner Lasertechnik GmbH, Vienna, Austria), and they were operated at a voltage of 7.5 V and 0.68 A. NMR samples were prepared by adding 50 μL of deuterated solvent to 800 μL of photoreaction mixture.

In Situ Fourier Transform Infrared (FTIR) Spectroscopy. In situ FTIR experiments were conducted using a ReactIR 702L system and DS AgX Comp probe from Mettler Toledo. A new spectrum was recorded once per minute over a range of 3000−650 cm^{-1}, which was set by the limitations of the instrument. The reaction was performed in a 250 mL three-neck round-bottom flask. The probe was held with a clamp stand at an angle and inserted into the rightmost neck. The same photoreactor setup was used, with the inlet and outlet tubes inserted into the left and center necks, respectively. Openings of the flask were wrapped in Parafilm to prevent evaporation and entry of moisture. The probe was calibrated every 48 h using ambient air.

When first inserting the probe into the solution, spectra were recorded every 10 s to ensure that the spectrum remained stable before beginning the reaction. After turning on the LEDs, the spectra were obtained at intervals of 1 min. Data was recorded in iC IR 7.1 software by Mettler Toledo.

The FTIR spectra of the pure substances (2BP, benzophenone, and lignin) were obtained by measuring the FTIR spectrum of a highly concentrated solution of 2BP or benzophenone. For lignin, dimethyl sulfoxide was used as a solvent to reach a high concentration. The FTIR spectrum of the pure solvent was subtracted.

Nuclear Magnetic Resonance (NMR). All NMR spectra were recorded on a Bruker Avance III HD (700 MHz ^1H) equipped with a QCI cryoprobe. The temperature was set to 25 °C, and the gradient strength was calibrated using a standard Bruker sample called doped water. The bulk solvent was MeCN, and 50 μL of deuterated MeCN was used to lock and shim the sample. The ^1H chemical shift is set according to the lock solvent, which is 1.93 ppm for MeCN. The choice of solvent might have an impact on the chemical shift. For example, aromatic substances as they might aggregate. The 1D spectra were recorded with a repetition delay of 15 s using solvent suppression, and the signal was accumulated 64 times.

For the diffusion experiments: A stimulated echo pulse sequence was used with a longitudinal eddy current delay, bipolar gradients, and solvent suppression. The repetition time was set to 15 s and 64 scans have been accumulated. The gradient duration was set to 4 ms (2 ms on each side), and the diffusion time was set to 50 ms. The gradient strength was varied in three steps (10, 30, and 50% of the maximum gradient strength of 0.7 T/m). The intensity of the peaks from the diffusion-weighted spectra are denoted I_{10}, I_{30}, and I_{50} according to the gradient strength. Homonuclear 2D NMR spectra were recorded with the pulse sequence dipsi2esfbgpph with 512 steps in the indirect dimension, a spectral width of 20 ppm, and a mixing time of 0.1 and 0.2 s.

For the difference in intensity with time and the diffusion-weighted spectra, the intensities were first binned with a binning step of 0.1 ppm. The Matlab (Mathworks) function mspeaks without denoising was applied to pick peaks.

Gas Chromatography−Mass Spectrometry (GC-MS). After the photoreactions, the solutions from each time point were filtered with a 0.45 μm nylon membrane filter in preparation for GC-MS analysis. Data were collected on an Agilent GC system 7890B coupled with an Agilent 5977A mass spectroscopy detector equipped with a moderately polar VF1701ms column (30 m × 0.25 mm × 0.25 μm) and analyzed with the provided software and databases. The injector port temperature was set at 280 °C (isothermal). The helium carrier gas was set to 0.8 mL/min of constant flow. The oven-temperature program was initially set to 40 °C with no hold and ramped to 280 °C at 5 °C/min with a hold of 1 min.

RESULTS AND DISCUSSION

One way to valorize technical lignin would be to cleave the linkages and form smaller oligomers or even monomers. However, analysis of reactions on technical lignin is inherently difficult due to the complex and heterogeneous structure of lignin itself. To facilitate the characterization, we studied first a simpler system with two aromatic rings linked with an ether

https://doi.org/10.1021/acssuschemeng.3c00097
ACS Sustainable Chem. Eng. 2023, 11, 4850−4859

bond, 2BP. The formation and deterioration of functional groups of 2BP and Kraft lignin were monitored in photoreactions with and without benzophenone. Three analysis methods i.e., GC-MS, NMR, and in situ FTIR, were employed to monitor the progress of the reactions. GC-MS was used to detect nonpolymerized products for the 2BP reactions. ^{1}H NMR was used to identify functional groups and their relative molecular size. However, 1D ^{1}H NMR lacks chemical shift separation in the aromatic region (6−8 ppm) for complex mixtures, complicating in-depth analysis. Furthermore, functional groups without attached hydrogens, such as substituted rings and oxidized functional groups, are not visible. The latter is complemented by in situ FTIR that can be used to detect C═O groups found in ketones and acids.

Benzophenone (the photosensitizer), 2BP, and lignin have chromophores that absorb light at 280 nm due to their conjugated π systems. This means that 2BP or lignin can react through direct photolysis or indirectly through the excitation of benzophenone. Additionally, the formed molecules can be electronically excited and react further. Acetonitrile (MeCN) was used as a solvent due to its low absorbance of the 280 nm light used in these photoreactions despite the low solubility of lignin.

First, we irradiated 2BP, and the obtained ^{1}H NMR spectra as a function of irradiation time are shown in Figure 1. The peak corresponding to the CH_2 group connected to the ether bond of 2BP at 5.2 ppm (indicated with 1, Figure 1) decayed within the 1st hour. Peaks at 4 ppm appeared and disappeared with irradiation time, which was also true for peaks in the aromatic region between 6 and 8 ppm. After 3 h of irradiation, a broad peak and many new small peaks became visible. Using GC-MS, several main products could be detected: benzyl alcohol, benzaldehyde, catechol, and 4-benzylbenzene-1,3-diol derivates. The latter is formed due to a rearrangement of the benzyloxy phenol which agrees with earlier results found in the literature.[29,30] The peaks close to 4 ppm which are visible at 0.5−1 h could correspond to the CH_2 linkage between the two rings in the 4-benzylbenzene-1,3-diol derivative. Upon the breakage of the ether bond, both benzaldehyde (indicated with 2, Figure 1) and benzyl alcohol (indicated with 3, Figure 1) appeared in the NMR spectra.

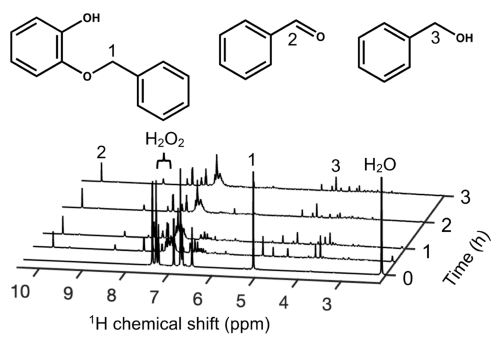

Figure 1. Molecular structures of 2-(benzyloxy)phenol (2BP), benzaldehyde, and benzyl alcohol from right to left at the top. ^{1}H NMR spectra of 2BP dissolved in MeCN as a function of irradiation time. Peaks labeled with 1, 2, and 3 correspond to the bonds of 2BP, benzaldehyde, and benzyl alcohol.

Figure 2 shows ^{1}H NMR spectra of a 2BP solution irradiated for 0, 1, and 3 h without (a) and with benzophenone (c). The peaks assigned to benzophenone arise between 7.5 and 8 ppm and overlap with the aromatic peaks of 2BP. Upon irradiation, the CH_2 group at the ether bond at 5.2 ppm was cleaved independently of the presence of the photosensitizer. The peak is still visible after 1 h (red) for the reaction with benzophenone in contrast to without the photosensitizer. Hence, the cleavage appeared to progress slower with the addition of benzophenone which was also observed for a much lower concentration of benzophenone (Figure S1). The slower reaction rate in the presence of benzophenone is likely caused by the fact that benzophenone absorbs photons at 280 nm and decreases transmittance through the solution, which probably reduces the rate at which 2BP absorbs photons.

An NMR spectrum consists of more than 100 000 data points (intensity versus chemical shift). The common practice of evaluating complex NMR spectra (e.g., from blood, urine, or food) has been to divide the spectrum into bins, each bin representing a sum of the intensities I over a range of chemical shifts. Hence, we binned the spectra to bins with a width of 0.01 ppm, a typical linewidth of a peak of a small molecule, and reduced the amount of data points from 100 000 to 800.

The net changes in the ^{1}H NMR spectra were visualized by subtracting the initial intensities from the intensities at 15 min, 1 h, and 3 h, as shown in Figure 2b,d. Due to the binning, the changes should be interpreted qualitatively and not quantita-

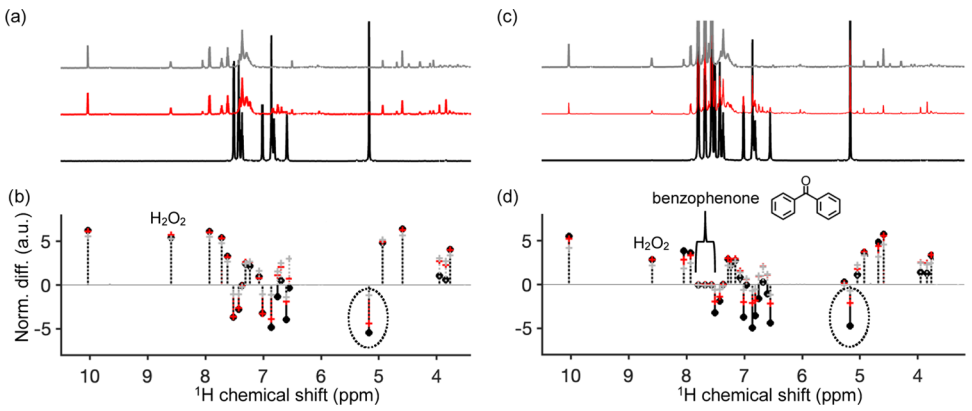

Figure 2. ^{1}H NMR spectra of 2BP reaction contents at 0 h (black), 1 h (red), and 3 h (gray) (a). The largest intensities have been cut for fitting. The spectra have been separated along the vertical axis to improve readability. Net changes in bin intensities calculated by subtraction of the initial intensities from the intensities at 15 min (gray), 1 h (red), and 3 h (black) (b). The same information is shown for the benzophenone samples in (c) and (d).

https://doi.org/10.1021/acssuschemeng.3c00097
ACS Sustainable Chem. Eng. 2023, 11, 4850−4859

tively. The dashed circles highlight the changes for the CH_2 group at the ether bond and corroborate that the cleavage occurred faster without benzophenone, indicated by the small change between the red line (1 h) and the black line (3 h) in Figure 2b. In both cases, H_2O_2 was formed.

The rate of formation of benzyl alcohol and benzaldehyde was proportional to the 2BP concentration i.e., "first-order" behavior, which was confirmed by GC-MS evaluation (Figure S2). Benzophenone is known to react to benzopinacol by a combination of two benzophenone triplet "radicals".[3] However, benzopinacol was not found in the GC-MS data, nor were any other apparent products of benzophenone. This is also in agreement with NMR spectra that showed no additional peaks after 3 h of irradiation in benzophenone dissolved in MeCN (Figure S3).

In situ FTIR measurements were recorded for photoreactions of 2BP, both with and without benzophenone. The aim of these experiments was to detect bonds that are not visible in the ^{1}H NMR spectra. The FTIR spectra of 2BP and benzophenone dissolved in MeCN and pure MeCN are shown in Figure 3a. To visualize the changes with time, which are

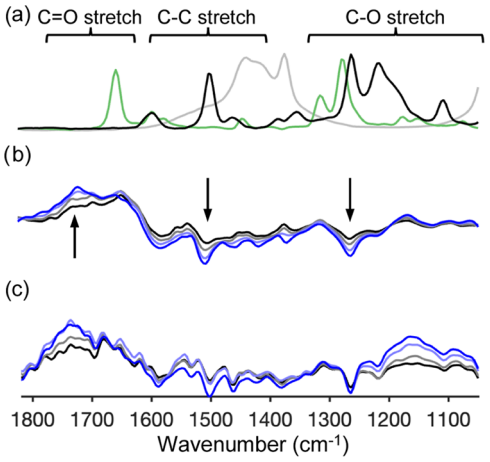

Figure 3. Plots of FTIR absorbance intensities over the range of wavenumbers with a sufficient signal-to-noise ratio. (a) Spectra for 2BP (black) dissolved in MeCN, benzophenone (green) dissolved in MeCN, and pure MeCN (gray). (b, c) Difference between the initial and measured absorbance over time after; 0.5 h (black), 1 h (gray), 2 h (light blue), and 3 h (blue). The spectra in (b) are for the reaction without benzophenone, and (c) are for the reaction with benzophenone. The *y*-axis is scaled to the maximum peak intensities.

small due to a concentration of 1 g/L, the wavenumber values at 0 h were subtracted from the values at each subsequent measurement taken throughout the reaction, resulting in plots showing the intensity differences between the spectra (Figure 3b,d).

The range of 1800−1100 cm^{-1} gave a sufficient signal-to-noise ratio for interpretation and is of interest because of the three main types of vibrational modes: C−C stretching in aromatics, C−O stretching in ethers, alcohols, and carboxylic acids, and C═O stretching in carbonyls. Unfortunately, the FTIR probe measures only up to 2500 cm^{-1} and information about O−H stretching in phenols, C−H stretching in alkene aromatics, and C−H stretching in aldehydes, could not be observed. Due to the complex mixture of reactants and products, we have based our interpretation on the type of bond and not on the typical fingerprint of an FTIR spectrum.

In 2BP reactions both with and without benzophenone, we observed a decrease in absorbance for the stretching of aromatic C−C bonds, and an increase in C═O stretching and C−O stretching absorbances. The increase in C═O signal agrees with the growth of the benzaldehyde peak at 10 ppm in ^{1}H NMR spectra in Figure 2b and the continuous formation of benzaldehyde observed with GC-MS (Figure S2). The decrease in aromatic signal confirmed 2BP being consumed (Figures 2d and S2). As 2BP reacts, the ether bond between the aromatic units is cleaved and apart from other molecules, benzyl alcohol is formed. Hence, we expected a decrease in the C−O stretching instead of an increase. This might be due to the benzyl alcohol and other C−O bonds absorbing FTIR differently. Furthermore, absorbances of H_2O_2 might appear in this region.[31]

Benzophenone seems to impact the reaction progress, but the overlap of benzophenone with other aromatic peaks in the ^{1}H NMR complicates the interpretation of how benzophenone enhances the reaction selectivity toward a desirable product. No trustworthy differences were observed from the FTIR. either. Furthermore, no changes in the benzophenone peak intensities were observed as shown in Figure 2d.

Polymerization is for most of the cases an unwanted reaction that might occur in photochemical reactions. Using diffusion NMR, bond cleavage and polymerization can be assessed through the obtained diffusion coefficients. However, for an accurate determination of diffusion coefficients for mixtures with similar chemical shifts and a broad size distribution, a large number of spectra with different diffusion-weighting need to be recorded with a very good signal-to-noise ratio. This requires long experimental times, and the recorded data needs to be fitted to multicomponent distributions or similar. Here we decided to use the ratio of the logarithmic intensity at 30% gradient strength $\ln(I_{30})$ versus the logarithmic intensity at 10% gradient strength $\ln(I_{10})$. This ratio can be used as a proxy of the apparent diffusion coefficient and was further normalized by the $\ln(I_{30})/\ln(I_{10})$ of 2BP. The diffusion coefficient is inversely proportional to the hydrodynamic radius based on the Stokes-Einstein relationship. Consequently, a normalized $\ln(I_{30})/\ln(I_{10})$ of 1 reflects the molecular size of 2BP. A lower value indicates a smaller molecular size and a larger one a bigger molecule regarding the radius. Overlapping peaks from different molecules will represent an averaged value. The results are shown in Figure 4a,d.

For benzaldehyde and benzyl alcohol, values lower than 1 were obtained which agrees with their smaller molecular size. The ratio of the hydroxyl group of 2BP resonating at 6.8 ppm was below 1 which might be explained by the intensity of the peak being modulated by the hydrogen on the hydroxyl group exchanging with the hydrogen of the water peak. The broad peak at 7.2 ppm appeared to belong to a larger molecule formed through polymerization. The same observations were found for the reactions with benzophenone (Figure 4d). Benzophenone showed a value below 1 because of a slightly smaller hydrodynamic radius than 2BP due to the shorter linkage. The peaks around 4 ppm seem also to be a product of polymerization.

Figure 4b,e represents the spectrum recorded with 10% gradient strength (black) overlapped with the corresponding ^{1}H NMR spectrum. For without and with benzophenone, there is an intensity loss despite choosing the same experimental settings (repetition time). This is caused by the delays in the

https://doi.org/10.1021/acssuschemeng.3c00097
ACS Sustainable Chem. Eng. 2023, 11, 4850−4859

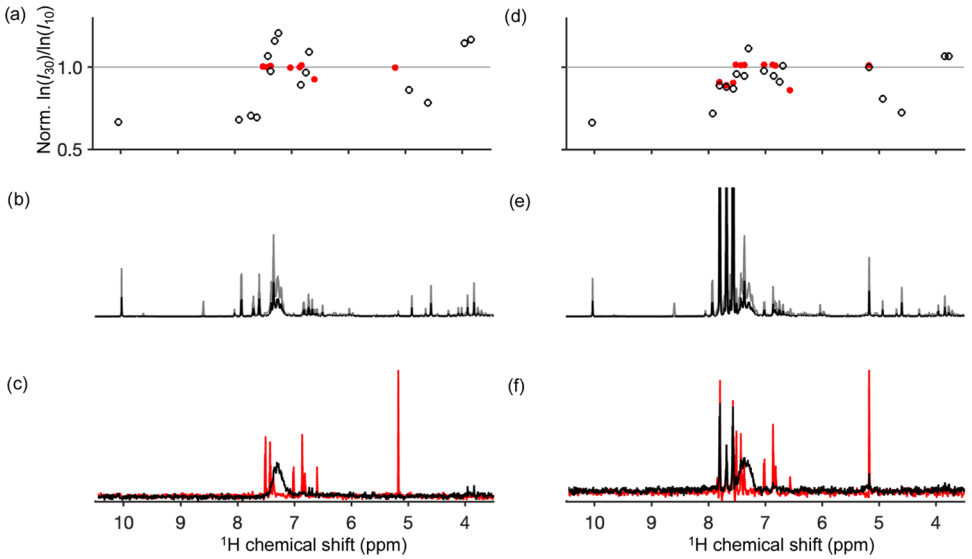

Figure 4. Normalized $\ln(I_{30})/\ln(I_{10})$ by dividing the $\ln(I_{30})$ by $\ln(I_{10})$ of 2BP for 2BP 0 h (red) and 1 h (black circles) in (a). Diffusion-weighted spectrum with 10% gradient strength for 2BP 1 h (black) and 1D ^{1}H spectrum for 2BP 1 h (gray) in (b). Diffusion-weighted spectrum with 50% gradient strength for 2BP 0 h (red) and 1 h (black) in (c). The same as (a) in (d) and (b) in (e) and (c) in (f) with the addition of benzophenone.

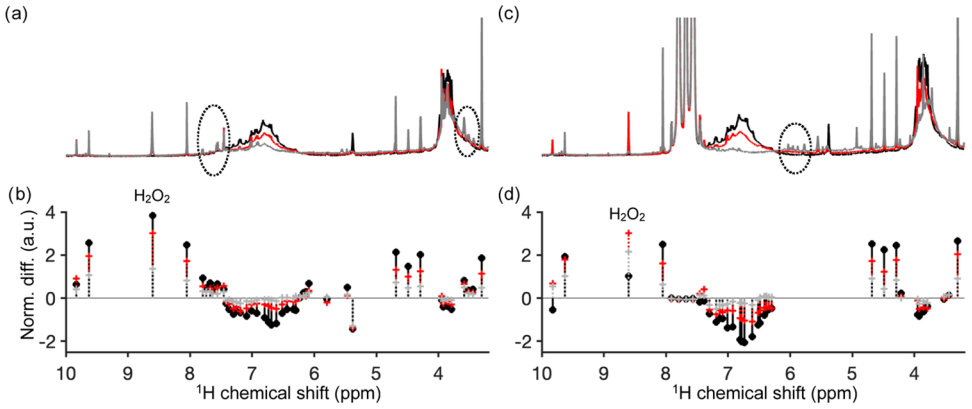

Figure 5. ^{1}H NMR spectra of lignin reaction contents at 0 h (black), 2 h (red), and 3 h (gray) (a). Net changes in bin intensities calculated by subtraction of the initial intensities from the intensities at 15 min (gray), 1 h (red), and 3 h (black) (b). The same information is shown for the benzophenone samples in (c) and (d).

pulse sequence that enable the estimation of the diffusion coefficient—peaks that correspond to functional groups with short relaxation times might have decayed before the signal is recorded. This has little impact on the results of the 2BP reactions but might play a crucial role in the reactions on lignin. As expected, the H_2O_2 peak at 8.5 ppm is not visible in the 10% gradient strength spectrum due to fast diffusion. Figure 4c,f shows the spectrum recorded with 50% gradient strength revealing slowly diffusing species like the broad peak at 7.2 ppm. For the 0 h samples, the peaks of 2BP and benzophenone were still visible due to their strong signal—the intensity at 50% gradient strength is only a tiny amount of the starting intensity. For the nonsensitized reaction, an attempt to estimate the diffusion coefficient from pseudo-2D datasets (Figure S4) was made and the results agree with the simpler methodology we used here.

The reactions with Kraft lignin were performed using the same conditions. The ^{1}H NMR spectra with and without benzophenone are shown in Figure 5a,c. The 0 h samples show the aromatic region between 6 and 8 ppm in which the G-units resonate. Furthermore, homonuclear 2D NMR revealed that the phenolic hydroxyl groups, the end groups which appear in DMSO above 8 ppm, arise in MeCN close to 6 ppm (Figure S5). These hydroxyl groups exchange with the water peak, indicated by a cross-peak in the 2D NMR spectrum. Another important region is the methoxy group region which overlaps with the CH_2 groups of the linkages.[32] The lignin peaks are in general broad due to lignin being a polymer and due to the heterogeneity of lignin—slightly different substitutions and linkages might alter the chemical shift.

After 2 h of irradiation as shown in Figure 5a,c (red), the intensity of the aromatic/phenolic and the methoxy/CH_2 region decreased. Simultaneously, new peaks appeared between 4 and 5 ppm, and above 8 ppm, independently on the presence of the photosensitizer. The reduction in the methoxy/CH_2 peaks at around 3.8 ppm differed upon the addition of benzophenone which is seen by a different peak shape (Figure 5a,c). This indicates the formation of different products. The difference-spectra in Figure 5b,d revealed that the intensities in the aromatic/phenolic regions decreased differently. A larger decrease below 7 ppm was observed upon the addition of benzophenone while for the nonsensitized

https://doi.org/10.1021/acssuschemeng.3c00097
ACS Sustainable Chem. Eng. 2023, 11, 4850−4859

reaction, the intensity decreased for all chemical shifts similarly. Additionally, new peaks appeared in the region between 7 and 8 ppm. Unfortunately, due to overlap with the benzophenone peaks, these peaks could not be detected for the reactions with benzophenone. The signal in the aromatic peak region (6−7 ppm) appeared to decrease faster in the reaction containing benzophenone, possibly due to an increased number of electrophilic attacks by singlet oxygen, which can be generated from energy transfer from triplet photosensitizers.[14,20,33,34] Furthermore, a lot of small peaks were noticed in the sample with benzophenone highlighted by a dashed circle in Figure 5c.

Methanol at 3.3 ppm is formed in all reactions. The peak at 8.05 ppm corresponds to formic acid and is produced through ring-opening reactions of lignin aromatic compounds in the presence of H_2O_2 in alkaline conditions,[22,23] but it is not clear whether the mechanism here is the same. Formic acid has also been used for lignin depolymerization, delignification, and hydrodeoxygenation, demonstrating its possible reactions with lignin itself.[35−37] In this reaction, it is unclear whether formic acid is reacting with lignin after it formed, but its involvement in other lignin reactions, even at room temperature, suggests the possibility. Around 9.6 ppm, a peak corresponding to an aldehyde group is growing in both reactions, which has been observed in other examples of lignin oxidation.[22,38]

As the reaction progressed, the formation of H_2O_2 was observed for both lignin and the 2BP reactions (Figure 2) independently of the presence of benzophenone. H_2O_2 is used in photooxidative water treatment processes because UV light causes photolysis of H_2O_2 into two hydroxyl radicals.[24,39] Hydroxyl radicals oxidize aromatic structures in lignin to produce smaller molecules, including carbonylic acid compounds, which are known from the research of advanced oxidation processes (AOPs) involving lignin, H_2O_2, and ultraviolet light.[24,39] H_2O_2 production has been reported with other triplet photosensitizers,[40] but there is no clear evidence here of a significantly higher H_2O_2 production rate in the samples containing benzophenone. The concentration of H_2O_2 is in the millimolar range and the intensities of the H_2O_2 peak varied unsystematically with irradiation time and repetitions. Hence, H_2O_2 might be involved in the reactions, but it is not driving the reaction. Miglbauer et al. have observed that lignin can act as a photocatalyst in the formation of H_2O_2.[41]

Photoreactions of Kraft lignin with and without benzophenone were also monitored with the in situ FTIR probe and the results are shown in Figure 6. The FTIR spectrum of lignin dissolved in DMSO agreed with the literature on FTIR on solid Kraft lignin.[42] For the reactions of Kraft lignin without benzophenone, there was an increase in absorbance in the regions corresponding with C−O and C═O stretching (Figure 6b). In the case of the lignin reactions with benzophenone, there was a decrease in absorbance over the aromatic range for both reaction repetitions, which was not observed in either repetition without benzophenone (Figure S6). The increase in C═O stretching might arise from the formation of formic acid and possibly from the oxidation of hydroxy groups, either phenolic or aliphatic forming ketones and aldehydes. The changes in the C−O stretching might be attributed to the formation of methanol. Furthermore, this region might overlap with absorbances from H_2O_2 that are formed during the reactions.[31]

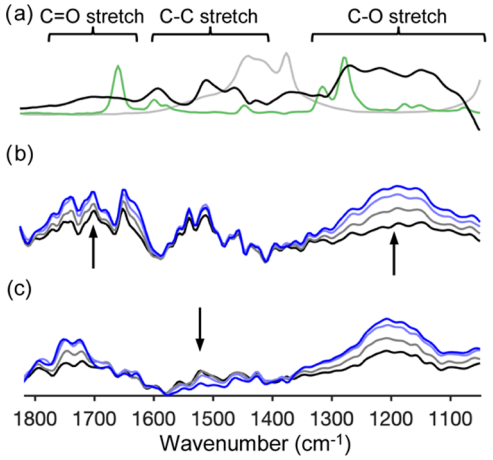

Figure 6. Plots of FTIR absorbance intensities over the range of wavenumbers with a sufficient signal-to-noise ratio. (a) Spectra for lignin (black) dissolved in DMSO, benzophenone (green) dissolved in MeCN, and pure MeCN (gray). (b, c) Difference between the initial and measured absorbance over time after; 0.5 h (black), 1 h (gray), 2 h (light blue), and 3 h (blue). The spectra in (b) are for the reaction without benzophenone, and (c) are for the reaction with benzophenone. The *y*-axis is scaled to the maximum peak intensities.

The normalized $\ln(I_{30})/\ln(I_{10})$ lignin dissolved in MeCN shows a distribution of ratios in the aromatic/phenolic and methoxy/CH_2 region around 2.3 as shown in Figure 7a. Upon the addition of benzophenone, the ratios increased slightly to 2.5 (Figure 7d). This is also confirmed for 2BP showing larger values when benzophenone is present (Figure 4d). This might indicate that benzophenone interacts with both 2BP and lignin for example through π-stacking. Upon irradiation, the ratios seem to decrease for the observable aromatic/phenolic peaks and methoxy/CH_2 peaks. However, these ratios should be seen as averaged values due to underlying broad peaks.

For formic acid (8.05 ppm) and methanol (3.3 ppm), values below 1 were obtained which agrees with being small molecules. The new aromatic peaks between 7.5 and 8 ppm in the nonsensitized samples belong to molecules that are smaller in size in comparison to lignin and they correlate with each other according to the 2D NMR (Figure S7). This suggests a molecule with two or three connected rings or a mixture of these smaller fragments. Some of these peaks showed correlations to the methoxy/CH_2 region, indicating that methoxy groups on the ring and/or the aromatic ring are close to a CH_2 group of a linkage. Interestingly, the new peaks between 4 and 5 ppm appeared to have a similar molecular size as 2BP and hence arise from smaller fragments. It is noteworthy to mention that peaks from CH groups of the different lignin linkages for example in β-O-4 that resonate between 4 and 5 ppm are not visible in the ^{1}H NMR spectrum. An explanation would be that the relaxation time of these groups is very short due to being incorporated inside a large molecule and hence not observable. The new peaks belong to smaller fragments that have longer relaxation times to be detected. The peak, in the 2D NMR, around 4.2 ppm correlates with peaks in the methoxy/CH_2 region and the water peak. This suggests a CH group connected to a CH_2 and a hydroxyl group as found in other lignin linkages (Figure S7). No clear correlations were found between the aromatic peaks and the peaks between 4 and 5 ppm. For these correlations to appear, the distance between the hydrogen atoms is

https://doi.org/10.1021/acssuschemeng.3c00097
ACS Sustainable Chem. Eng. 2023, 11, 4850−4859

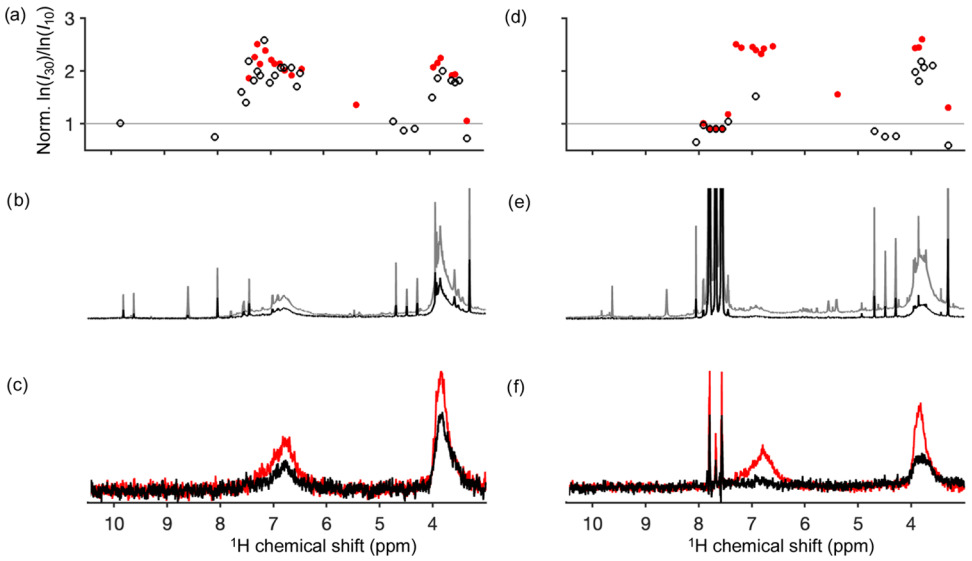

Figure 7. Normalized $\ln(I_{30})/\ln(I_{10})$ by dividing the $\ln(I_{30})$ by $\ln(I_{10})$ of lignin for lignin 0 h (red) and 2 h (black circles) (a). Diffusion-weighted spectrum with 10% gradient strength for lignin 2 h (black) and 1D ^{1}H spectrum for lignin 2 h (gray) (b). Diffusion-weighted spectrum with 50% gradient strength for lignin 0 h (red) and 2 h (black) (c). The same as (a) in (d), (b) in (e), and (c) in (f) with the addition of benzophenone.

important—in general the shorter the more efficient—and the rotational mobility of the functional group. The presence of oxidized functional groups without hydrogen atoms between these groups prolongs the distance. It seems however possible that the aromatic peaks and the peaks between 4 and 5 ppm are part of the same fragments. Unfortunately, the concentration of the solution is too low to record ^{13}C NMR, which would have eased further interpretation. The peaks between 4 and 5 ppm appeared in the sensitized reaction and are more intense compared to the lignin peak intensities at 0 h. Furthermore, 2D NMR for sensitized reactions could not be recorded in good quality due to the intense benzophenone peaks. Hence, it is not clear if there are new aromatic peaks present although we anticipate them to be there.

Figure 7b,e represents the spectrum recorded with 10% gradient strength (black) overlapped with the corresponding ^{1}H NMR spectrum. For without and with benzophenone, there is a greater intensity loss compared to 2BP suggesting that parts of the lignin might have very short relaxation times. It is also noteworthy that the loss in intensity is more pronounced for the reactions with benzophenone. In addition, there is a "baseline" for the ^{1}H NMR spectrum (gray) which cannot be corrected for. This is an indication of the formation of large molecules due to polymerization which also occurred for 2BP. Due to the delays in the pulse sequence, this broad underlying signal is not observed in the diffusion-weighted spectra. As for the 2BP reactions, the H_2O_2 peak at 8.5 ppm was no longer observed in the 10% gradient strength spectrum due to fast diffusion. This is most likely also true for the aldehyde peak at 9.7 ppm indicating that this functional group is part of a small molecule.

Figure 7c,f shows the spectrum recorded with 50% gradient strength revealing the slowly diffusing parts of lignin for 0 h (red) and 2 h (black). Comparing these two spectra (black), the different shape of the methoxy/CH_2 region is obvious. These results agree in addition with the faster decay of the aromatic region for the addition of benzophenone. However, the methoxy/CH_2 peak is still visible, suggesting that the aromatic peak should still there but might be too broad to be observed. For the nonsensitized reaction, the estimation of the diffusion coefficient from pseudo-2D datasets also agrees with the simpler methodology (Figure S8). Small aromatic molecules could however not be identified with GC-MS, indicating that there is a mixture of smaller fragments with concentrations too low to be identified.

CONCLUSIONS

The results of nonsensitized and benzophenone-sensitized reactions of 2BP and Kraft lignin in MeCN showed that benzophenone affects reactions of 2BP and Kraft lignin differently. In 2BP, photoreactions were slowed down while for lignin the reactions progressed faster. We can conclude that 2BP does not give a complete picture of how ether bonds in lignin degrade. Changes in intensity, peak shapes, and linewidth evidenced that bond cleavage and polymerization occurred.

The faster decrease in the broad aromatic/phenolic ^{1}H NMR peak for the phenolic hydroxyl group region observed in the benzophenone reaction could be caused by one of two mechanisms. Benzophenone could be causing an increase in the concentration of reactive oxygen species via triplet sensitization. These reactive oxygen species would then react with lignin. Alternatively, benzophenone could participate in hydrogen abstraction, leading to subsequent reactions. Overall, also for lignin, smaller fragments and molecules were formed besides repolymerization.

Photochemical reactions of 2BP and lignin are complex and involve bond cleavage, bond formation, and rearrangement reactions. This complexity makes it challenging to develop a mechanistic understanding of the reactions. Benzophenone has different impacts on the reactions and further optimization is needed to tune the occurring reactions in favor of depolymerization to valorize lignin.

The observation that a photosensitizer can participate in lignin reactions opens questions about the use of other types of photosensitizers. The effects of triplet state lifetime, sensitization, energy transfer, hydrogen transfer, electron transfer, and

https://doi.org/10.1021/acssuschemeng.3c00097
ACS Sustainable Chem. Eng. 2023, 11, 4850−4859

concentration of reactive oxygen species will be further investigated for photochemical lignin valorization research.

■ ASSOCIATED CONTENT

Supporting Information

The Supporting Information is available free of charge at https://pubs.acs.org/doi/10.1021/acssuschemeng.3c00097.

NMR results of previous 2BP reactions, GC-MS results of 2BP reactions, ^{1}H NMR spectra of benzophenone before/after irradiation, 2D NMR of lignin, repetitions of FTIR experiments, and diffusion coefficient plot (PDF)

■ AUTHOR INFORMATION

Corresponding Author

Diana Bernin − *Chemistry and Chemical Engineering, Chalmers University of Technology, 41296 Gothenburg, Sweden;* orcid.org/0000-0002-9611-2263; Email: diana.bernin@chalmers.se

Authors

Alexander Riddell − *Chemistry and Chemical Engineering, Chalmers University of Technology, 41296 Gothenburg, Sweden*

Jonna Hynynen − *Chemistry and Chemical Engineering, Chalmers University of Technology, 41296 Gothenburg, Sweden;* orcid.org/0000-0003-4543-928X

Francisco Baena-Moreno − *Chemistry and Chemical Engineering, Chalmers University of Technology, 41296 Gothenburg, Sweden*

Abdenour Achour − *Chemistry and Chemical Engineering, Chalmers University of Technology, 41296 Gothenburg, Sweden*

Gunnar Westman − *Chemistry and Chemical Engineering, Chalmers University of Technology, 41296 Gothenburg, Sweden;* orcid.org/0000-0001-6150-5203

Jim Parkås − *Södra Skogsägarna ekonomisk förening, Södra Innovation, 43286 Väröbacka, Sweden*

Complete contact information is available at: https://pubs.acs.org/10.1021/acssuschemeng.3c00097

Notes

The authors declare no competing financial interest.

■ ACKNOWLEDGMENTS

The Swedish NMR Centre is acknowledged for spectrometer time. The authors acknowledge the funding from Södra's forskningsstiftelse (2019-102 and 2020-168), the Swedish Research Council (2019-04066), and FORMAS (FR-2021/0005).

■ REFERENCES

(1) Ragauskas, A. J.; Beckham, G. T.; Biddy, M. J.; Chandra, R.; Chen, F.; Davis, M. F.; Davison, B. H.; Dixon, R. A.; Gilna, P.; Keller, M.; Langan, P.; Naskar, A. K.; Saddler, J. N.; Tschaplinski, T. J.; Tuskan, G. A.; Wyman, C. E. Lignin Valorization: Improving Lignin Processing in the Biorefinery. *Science* **2014**, *344*, No. 1246843.

(2) Pape, M. Industrial Applications of Photochemistry. *Pure Appl. Chem.* **1975**, *41*, 535−558.

(3) Scaiano, J. *Photochemistry Essentials*; American Chemical Society: Washington, DC, 2022.

(4) Li, S.-H.; Liu, S.; Colmenares, J. C.; Xu, Y.-J. A Sustainable Approach for Lignin Valorization by Heterogeneous Photocatalysis. *Green Chem.* **2016**, *18*, 594.

(5) Ksibi, M.; Amor, S. B.; Cherif, S.; Elaloui, E.; Houas, A.; Elaloui, M. Photodegradation of Lignin from Black Liquor Using a UV/TiO_2 System. *J. Photochem. Photobiol. A* **2003**, *154*, 211−218.

(6) Xiang, Z.; Han, W.; Deng, J.; Zhu, W.; Zhang, Y.; Wang, H. Photocatalytic Conversion of Lignin into Chemicals and Fuels. *ChemSusChem* **2020**, *13*, 4199−4213.

(7) Chen, H.; Wan, K.; Zheng, F.; Zhang, Z.; Zhang, Y.; Long, D. Mechanism Insight into Photocatalytic Conversion of Lignin for Valuable Chemicals and Fuels Production: A State-of-the-Art Review. *Renewable Sustainable Energy Rev.* **2021**, *147*, No. 111217.

(8) Michelin, C.; Hoffmann, N. Photosensitization and Photocatalysis - Perspectives in Organic Synthesis. *ACS Catal.* **2018**, *8*, 12046−12055.

(9) Cao, L.; Yu, I. K. M.; Liu, Y.; Ruan, X.; Tsang, D. C. W.; Hunt, A. J.; Ok, Y. S.; Song, H.; Zhang, S. Lignin Valorization for the Production of Renewable Chemicals: State-of-the-Art Review and Future Prospects. *Bioresour. Technol.* **2018**, *269*, 465−475.

(10) Hynynen, J.; Riddell, A.; Achour, A.; Takacs, Z.; Wallin, M.; Parkås, J.; Bernin, D. 'Lignin and Extractives First' Conversion of Lignocellulosic Residual Streams Using UV Light from LEDs. *Green Chem.* **2021**, *23*, 8251−8259.

(11) Elliott, L. D.; Kayal, S.; George, M. W.; Booker-Milburn, K. Rational Design of Triplet Sensitizers for the Transfer of Excited State Photochemistry from UV to Visible. *J. Am. Chem. Soc.* **2020**, *142*, 14947−14956.

(12) Wilkinson, F.; Kelly, G. P.; Ferreira, L. F. V.; Freire, V. M. M. R.; Ferreira, M. I. Benzophenone Sensitization of Triplet Oxazine and of Delayed Fluorescence by Oxazine in Acetonitrile Solution. *J. Chem. Soc., Faraday Trans.* **1991**, *87*, 547−552.

(13) Taylor, L. J.; Tobias, J. W. Accelerated Photo-Oxidation of Polyethylene. I. Screening of Degradation-Sensitizing Additives. *J. Appl. Polym. Sci.* **1977**, *21*, 1273−1281.

(14) Forsskåhl, I. Aspects of Photosensitized Lignin Oxygenation. *J. Photochem.* **1984**, *25*, 197−209.

(15) Luo, N.; Wang, M.; Li, H.; Zhang, J.; Hou, T.; Chen, H.; Zhang, X.; Lu, J.; Wang, F. Visible-Light-Driven Self-Hydrogen Transfer Hydrogenolysis of Lignin Models and Extracts into Phenolic Products. *ACS Catal.* **2017**, *7*, 4571−4580.

(16) Cao, Y.; Wang, N.; He, X.; Li, H. R.; He, L. N. Photocatalytic Oxidation and Subsequent Hydrogenolysis of Lignin β-O-4 Models to Aromatics Promoted by in Situ Carbonic Acid. *ACS Sustainable Chem. Eng.* **2018**, *6*, 15032−15039.

(17) Zhang, C.; Wang, F. Catalytic Lignin Depolymerization to Aromatic Chemicals. *Acc. Chem. Res.* **2020**, *53*, 470−484.

(18) Hosono, K.; Kanazawa, A.; Mori, H.; Endo, T. Photodegradation of Cellulose Acetate Film in the Presence of Benzophenone as a Photosensitizer. *J. Appl. Polym. Sci.* **2007**, *105*, 3235−3239.

(19) Prado, R.; Erdocia, X.; Labidi, J. Effect of the Photocatalytic Activity of TiO_2 on Lignin Depolymerization. *Chemosphere* **2013**, *91*, 1355−1361.

(20) Gorman, A. A.; Hamblett, I.; Rodgers, M. A. J. Time-Resolved Luminescence Measurements of Triplet-Sensitized Singlet-Oxygen Production: Variation in Energy-Transfer Efficiencies. *J. Am. Chem. Soc.* **1984**, *106*, 4679−4682.

(21) Kim, K. H.; Kim, C. S. Recent Efforts to Prevent Undesirable Reactions From Fractionation to Depolymerization of Lignin: Toward Maximizing the Value From Lignin. *Front. Energy Res.* **2018**, *6*, 92.

(22) Xiang, Q.; Lee, Y. Y. Oxidative Cracking of Precipitated Hardwood Lignin by Hydrogen Peroxide. *Appl. Biochem. Biotechnol., Part A* **2000**, *84*−*86*, 153−162.

(23) He, W.; Gao, W.; Fatehi, P. Oxidation of Kraft Lignin with Hydrogen Peroxide and Its Application as a Dispersant for Kaolin Suspensions. *ACS Sustainable Chem. Eng.* **2017**, *5*, 10597−10605.

(24) Makhotkina, O. A.; Preis, S. V.; Parkhomchuk, E. V. Water Delignification by Advanced Oxidation Processes: Homogeneous and

Heterogeneous Fenton and H_2O_2 Photo-Assisted Reactions. *Appl. Catal., B* **2008**, *84*, 821−826.
(25) Neumann, M. G.; De Groote, R. A. M. C.; Machado, A. E. H. Flash Photolysis of Lignin: Part 1. Deaerated Solutions of Dioxane-Lignin. *Polym. Photochem.* **1986**, *7*, 401−407.
(26) Neumann, M. G.; De Groote, R. A. M. C.; Machado, A. E. H. Flash Photolysis of Lignin: II-Oxidative Photodegradation of Dioxane-Lignin. *Polym. Photochem.* **1986**, *7*, 461−468.
(27) *Facts and Key Figures Swedish Forest-Based Industry* Swedish Forest Industries Federation: Stockholm, Sweden; 2022.
(28) Riddell, A.; Kvist, P.; Bernin, D. A 3D Printed Photoreactor for Investigating Variable Reaction Geometry, Wavelength, and Fluid Flow. *Rev. Sci. Instrum.* **2022**, *93*, No. 084103.
(29) Pan, Z.; Puente-Urbina, A.; Bodi, A.; van Bokhoven, J. A.; Hemberger, P. Isomer-Dependent Catalytic Pyrolysis Mechanism of the Lignin Model Compounds Catechol, Resorcinol and Hydroquinone. *Chem. Sci.* **2021**, *12*, 3161−3169.
(30) Weigert, F. J. HZSM-5-Catalyzed Dihydroxybenzene Equilibration. *J. Org. Chem.* **1987**, *52*, 921−923.
(31) Zins, E. L.; Krim, L. Hydrogenation Processes from Hydrogen Peroxide: An Investigation in Ne Matrix for Astrochemical Purposes. *RSC Adv.* **2014**, *4*, 22172−22180.
(32) Crestini, C.; Lange, H.; Sette, M.; Argyropoulos, D. S. On the Structure of Softwood Kraft Lignin. *Green Chem.* **2017**, *19*, 4104−4121.
(33) Hwang, K. O.; Lucia, L. A. Fundamental Insights into the Oxidation of Lignocellulosics Obtained from Singlet Oxygen Photochemistry. *J. Photochem. Photobiol. A* **2004**, *168*, 205−209.
(34) Machado, A. E. H.; Gomes, A. J.; Campos, C. M. F.; Terrones, M. G. H.; Perez, D. S.; Ruggiero, R.; Castellan, A. Photoreactivity of Lignin Model Compounds in the Photobleaching of Chemical Pulps 2. Study of the Degradation of 4-Hydroxy-3-Methoxy-Benzaldehyde and Two Lignin Fragments Induced by Singlet Oxygen. *J. Photochem. Photobiol. A* **1997**, *110*, 99−106.
(35) Rahimi, A.; Ulbrich, A.; Coon, J. J.; Stahl, S. S. Formic-Acid-Induced Depolymerization of Oxidized Lignin to Aromatics. *Nature* **2014**, *515*, 249−252.
(36) Xu, W.; Miller, S. J.; Agrawal, P. K.; Jones, C. W. Depolymerization and Hydrodeoxygenation of Switchgrass Lignin with Formic Acid. *ChemSusChem* **2012**, *5*, 667−675.
(37) Nguyen, J. D.; Matsuura, B. S.; Stephenson, C. R. J. A Photochemical Strategy for Lignin Degradation at Room Temperature. *J. Am. Chem. Soc.* **2014**, *136*, 1218−1221.
(38) Rodrigues Pinto, P. C.; Borges Da Silva, E. A.; Rodrigues, A. E. Insights into Oxidative Conversion of Lignin to High-Added-Value Phenolic Aldehydes. *Ind. Eng. Chem. Res.* **2011**, *50*, 741−748.
(39) Kang, J.; Irmak, S.; Wilkins, M. Conversion of Lignin into Renewable Carboxylic Acid Compounds by Advanced Oxidation Processes. *Renewable Energy* **2019**, *135*, 951−962.
(40) Guo, X.; Li, X.; Liu, X. C.; Li, P.; Yao, Z.; Li, J.; Zhang, W.; Zhang, J. P.; Xue, D.; Cao, R. Selective Visible-Light-Driven Oxygen Reduction to Hydrogen Peroxide Using BODIPY Photosensitizers. *Chem. Commun.* **2018**, *54*, 845−848.
(41) Miglbauer, E.; Gryszel, M.; Głowacki, E. D. Photochemical Evolution of Hydrogen Peroxide on Lignins. *Green Chem.* **2020**, *22*, 673−677.
(42) Ponomarenko, J.; Dizhbite, T.; Lauberts, M.; Viksna, A.; Dobele, G.; Bikovens, O.; Telysheva, G. Characterization of Softwood and Hardwood Lignoboost Kraft Lignins with Emphasis on Their Antioxidant Activity. *BioResources* **2014**, *9*, 2051−2068.

https://doi.org/10.1021/acssuschemeng.3c00097
ACS Sustainable Chem. Eng. 2023, 11, 4850−4859